ORGANIC-INORGANIC HYBRIDS PREPARED FROM ALKYL PHOSPHONIUM SALTS INTERCALATED MONTMORILLONITES

SAHELI GANGULY*, #KAUSIK DANA*, TAPAN K. PARYA**, TAPAS K. MUKHOPADHYAY*, SANKAR GHATAK*

*Advanced Clay and Traditional Ceramics Division Central Glass and Ceramic Research Institute, CSIR, Kolkata-700032, India
**Department of Chemical Technology, University of Calcutta, 92, A.P.C. Road, Kolkata-700009, India

#E-mail: kdana@cgcri.res.in

Submitted June 14, 2012; accepted October 21, 2012

Keywords: Montmorillonite, Alkyl phosphonium salts, Organic-Inorganic Hybrids, Interlayer spacing, Organic loading

Present investigation is focused on systematic and detailed characterization of alkyl phosphonium intercalated montmorillonite (MMT). The objective of the work is to provide a better understanding of the specific changes in properties of the hybrid material with changes in structure of incoming organic cations. In the present work, Na-MMT was intercalated with phosphonium salts of two different cationic head compositions namely alkyl triphenyl and alkyl tributyl groups. Length of alkyl chain was also varied. Resultant organic-inorganic hybrids were characterized by X-ray diffraction (XRD), Transmission electron microscopy (TEM), Thermogravimetry (TG) and Fourier transformed infrared spectroscopy (FTIR). Effective volume occupied by the cationic heads influenced interlayer arrangements. Intercalated MMT with two different cationic heads behaved differently in relation to thermal decomposition patterns. Possible explanation was given based on hybridization of bonds. Van der Waals attachment of alkyl chains influenced the interlayer stacking and organic loading. Attempts were made to correlate the changes in properties of intercalated MMT with the structural aspects of incoming organic cations.

INTRODUCTION

Organically modified MMT is an important organic-inorganic hybrid derived from intelligent combination of two dissimilar components, viz., MMT and organic molecules. The clay component of this hybrid provides a layer structure with remarkable surface property, which can be engineered by organic molecules. These hybrid materials have received attention because it affords new applications in different potential fields. During the last decade, modified MMT as nanometer-size fillers of organic polymers are increasingly used due to its superior physical, mechanical and thermal properties than conventional mineral-filled composites or unfilled polymers [1-5]. The automotive, aerospace and packaging industries view these clay mineral filled polymer nanocomposites as promising materials for the 21st century. These intercalated MMT can also be used as adsorbents for organic pollutants, rheological control agents, electric appliances, in waste water treatment, as thickening and gelling agent in paints, lubricants, ointments, as drug delivery vehicle etc [4, 6-7]. MMT is 2:1 layered silicate mineral with high cation exchange property and very high aspect ratio. The thickness of a single MMT platelet is ~ 0.96nm and lateral dimension of few hundred nanometers [8]. Intercalation reaction proceeds by replacing interlayer charge-balancing exchangeable cations of MMT by long chain organic cations. Key aspect of this organic treatment is to alter the hydrophilic nature of clay surface and enhance interlayer spacing of MMT. Quite a few investigations on different properties of MMT and intercalation of different organic molecules within MMT have been carried out [9-14]. Analysis revealed that among the clay minerals, MMT has been used extensively to prepare organophillic clays because of its excellent properties such as high cation exchange capacity, large surface area, swelling behavior and adsorption capacities. Earlier studies found that alkyl phosphonium intercalated MMT survive at much higher temperatures and were proven to be used in high melting point polymer/clay mineral composites [15-20]. A few studies with alkyl ammonium salts have proved that interlayer structure of organics is an important factor to guide the properties of intercalated MMT [21-22]. Thorough knowledge on the structure-property relationship of intercalates and intercalated MMT is necessary in the context of its different potential application purposes. Systematic investigations related to changes of cationic head composition of incoming organic cations and their effect on the properties of the intercalated MMT has not yet been explored by earlier authors. To fill up the gap current experiments were

designed. MMT was intercalated with phosphonium cations of two different cationic head compositions (alkyl triphenyl and alkyl tributyl head) with varying chain length and complete characterizations of these intercalated MMT were done. Attempt was made to realize how cationic head group structure of phosphonium intercalates influence interlayer spacing enhancements, interlayer arrangements, organic loading, and thermal decompositions of the modified MMT which might widen the applicability of the material. The work on structure - property relationship of intercalates and intercalated MMT has a great relevance in focusing the role of above said hybrid as nanofillers in the clay mineral based polymer nanocomposites.

EXPERIMENTAL

Materials

MMT 'M' (PGV, Nanocor, USA) was used in this study (in sodium form) because of its high cation exchange capacity (CEC) which was primarily responsible for effective intercalation. CEC was measured using EDTA-titrimetric method based on alkali or alkaline earth cations exchange principle [23-26]. The value of CEC was 88 C.mol.kg^{-1}. Intercalates were obtained from Sigma-Aldrich, USA. Intercalates used, belonged to two broad sets namely alkyl triphenyl phosphonium (Ph_3C_n) and alkyl tributyl phosphonium (Bu_3C_n). In one group, intercalates were carefully selected with three phenyl rings and one alkyl group attached to phosphorous. The alkyl group was varied as CH_3, C_2H_5, C_3H_7, and $C_{12}H_{25}$, and marked as Ph_3C_1, Ph_3C_2, Ph_3C_3, and Ph_3C_{12}. In Bu_3C_4, Bu_3C_{14}, and Bu_3C_{16}, three butyl groups with one varying alkyl chain such as C_4H_9, $C_{14}H_{29}$, and $C_{16}H_{33}$, was attached with phosphorous. The above said series of alkyl-triphenyl and alkyl-tributyl phosphonium salts were selected for intercalation of MMT.

Methods

Intercalation

Intercalation procedure was as follows. MMT was used in sodium (Na^+) form. 1 g clay was dispersed in 250 ml deionized water with sonication (0.5 W.cm^{-2}). 200 ml intercalate solution was added drop wise into this suspension with constant stirring. The entire intercalation was carried out at ~ 70 - 80°C. The reaction mixture was kept overnight for settling. The supernatant water with excess surfactant was decanted and the flock was redispersed in water. The process was repeated three times. Product was filtered under suction and washed with 2000 ml hot water. The collected product was dried at 70°C in vacuum for ~24 h. The dried product was ground in an agate mortar and kept in sealed glass bottles.

Characterization of intercalated MMT

Interlayer spacing and arrangements were deduced from X-ray diffraction analysis (XRD) and verified from transmission electron microscopic (TEM) analysis. Thermal nature and organic loading were calculated from thermogravimetric analysis (TGA). Characteristic stretching and bending vibration bands were identified from FTIR analysis.

XRD analysis

The studies on basal spacing of MMT and intercalated MMT done in XPERT-PRO (PANALYTICAL) diffractometer .The system was operated at 30 mA, 40 kV between 2.0 to 10.0 (2θ) at a step of 0.05.

TEM analysis

Transmission electron microscopy studies of the raw and intercalated clay mineral were performed using a Tecnai G^2 30 S–T transmission electron microscope. The filament of the instrument is of lanthanum hexaboride (LaB_6). The instrument has a line resolution and point resolution 1.4 Å and 2.0 Å respectively and has been operated at 300 kV during the investigation.

TG analysis

TG-DTG analyses of the samples were obtained using instrument NETZSCH STA 409 C. The system was operated at a heating rate 10.0°C.min^{-1} from 40°C up to 1050°C in presence of air with ~12 mg sample in alumina crucible.

FTIR analysis

Fourier transform infrared spectra (FTIR) have been measured with the SHIMADZU, FTIR-8300, Japan, using KBr pellet.

RESULTS AND DISCUSSIONS

XRD and TEM studies

Interlayer arrangement of organic cations can be elucidated by X-ray diffraction analysis. Experimental MMT (M) showed d_{001} ~1.25 nm (Figure 1), which is generally observed in Na^+ MMT [27]. The smectite group of minerals show variable integral series of basal spacing (d_{00l}) which is dependent upon the size of exchangeable cations and on the degree of hydration of the cation [27-30]. After ethylene glycol treatment, the peak shifted to 1.7 nm (Figure 2) which is also characteristic of Na^+-MMT. Intercalation by ion exchange with the alkyl phosphonium cations increased interlayer spacing (d_{001})

of M (Figure 3 and Figure 4). The increase in d_{001} was due to removal of smaller hydrated interlayer cation by bulky organic cations during ion exchange reaction [27]. Interlayer spacing 'Δ' (Δ = thickness of organic layer sandwiched between two clay layers) was calculated (Table 1) by subtracting the average thickness of one MMT layer (0.96 nm) from d_{001}. XRD plots showed increment of interlayer spacing with alkyl chain length for both the cationic head group structures (Figure 3 and Figure 4). But peak patterns and interlayer arrangements varied in a considerable extent with the cationic head group compositions. For M-Ph_3C_1 to M-Ph_3C_3, d_{001} spacing increased from 1.70 nm to 1.81 nm. The peaks were sharp and precise (Figure 3). Interlayer spacing calculation disclosed that all these cations took bilayer arrangements with in interlayer spaces of MMT (Table 1). In M-Ph_3C_{12}, d_{001} spacing increased up to 2.7 nm but the peak was broad with a little hump at d_{001} spacing 2.15 nm (Figure 3). d_{001} spacing values at 2.7 nm and 2.1 nm depicted that Ph_3C_{12} took parafinnic arrangements. In paraffinic interlayer arrangements, organic cations stand more erect creating an angle with the clay surface unlike of mono- and bilayer arrangements where molecules are laterally arranged. Generally long chain organic molecules took this type of arrangements to achieve higher van der Waals stability [4, 28]. Due to long alkyl

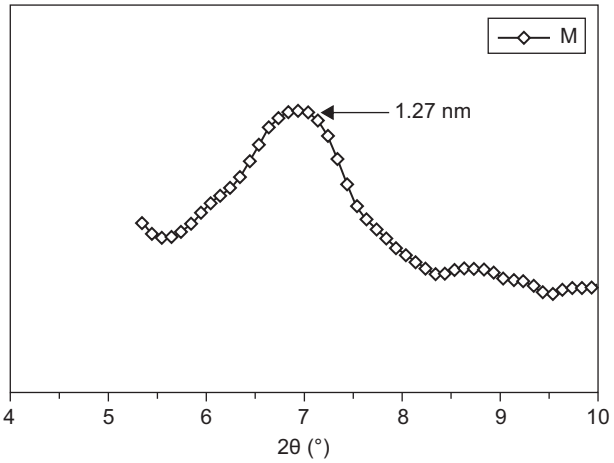

Figure 1. XRD plot of untreated M.

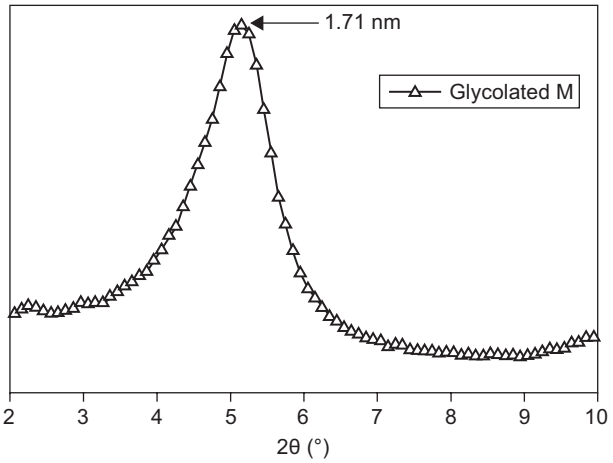

Figure 2. XRD plot of glycolated M.

Table 1. XRD results of intercalated Mt.

Intercalated M	d spacing (nm)	Δ = Interlayer spacing (nm)	Interlayer arrangement
M-Ph_3C_1	1.70	0.74	Bilayer
M-Ph_3C_2	1.77	0.81	Bilayer
M-Ph_3C_3	1.81	0.85	Bilayer
M-Ph_3C_{12}	2.7, 2.15	1.74, 1.19	Paraffinic
M-Bu_3C_{14}	2.6	1.64	Paraffinic
M-Bu_3C_{16}	2.7	1.74	Paraffinic
M-Bu_3C_4	2.0, 1.6	1.04	Paraffinic

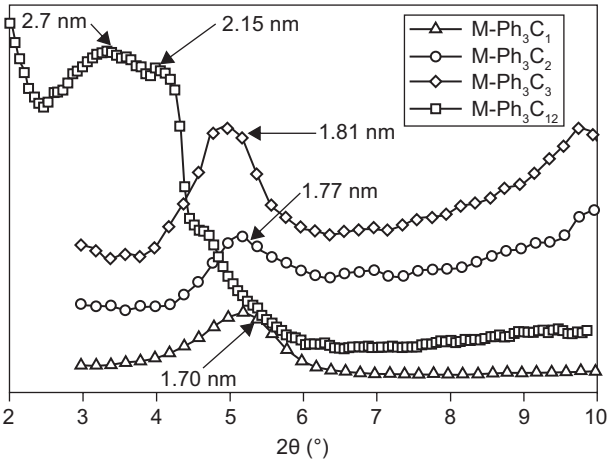

Figure 3. XRD plot of alkyl triphenyl phosphonium intercalated M.

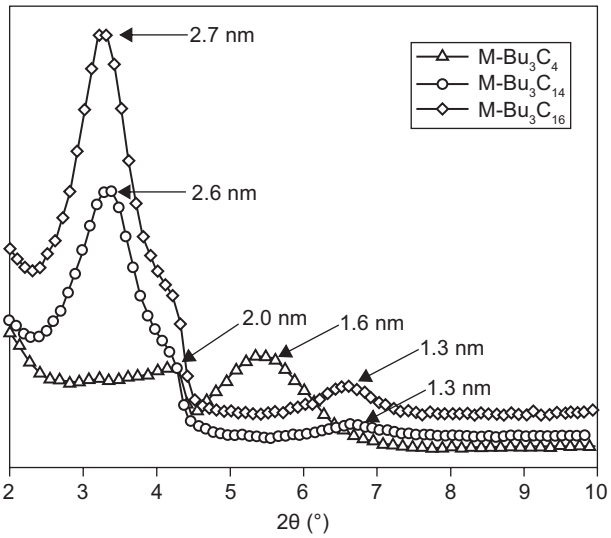

Figure 4. XRD plot of alkyl tributyl phosphonium intercalated M.

chain, Ph_3C_{12} took above said arrangements. But tilting angle of inserted molecules with the clay surface were different creating interlayer expansions in different extent. Superposition of reflections corresponding to these different interlayer distances created multiple wide peaks. Coexistence of different interlayer arrangements or layer heterogeneity was observed at C_{12} alkyl chain length of alkyl triphenyl cationic head group. But nature of XRD peaks of alkyl tributyl head group were unlike that of the previous one (Figure 4). From M-Bu_3C_4 to M-Bu_3C_{16}, the peaks were sharp indicating interlayer heterogeneity was less up to C_{16} alkyl chain length compared to that of alkyl triphenyl head group. d_{001} spacing was 2.0 nm to 2.7 nm which disclosed that paraffinic layer arrangement was adopted within interlayer space of MMT. Another prominent peak appeared with in 1.3 - 1.6 nm region for all the intercalated MMT in alkyl tributyl head group set. So, some partially intercalated layers with lateral monolayer arrangement were also there in M-Bu_3C_4 to M-Bu_3C_{16}. Organic loading calculation from TG plot (Table 2) revealed that with only 9 wt. % organic loading, M-Bu_3C_4 showed interlayer expansion up to 2.0 nm whereas M-Ph_3C_3 showed 1.81 nm d_{001}spacing with 28 wt. % organic loading. This can be due to the higher effective volume occupied by three butyl chain of alkyl tributyl head group within interlayer space compared to that of three phenyl ring of alkyl triphenyl head. These findings from XRD were supported by TEM analysis. The most widely used technique to determine the structure of the intercalated clay mineral is XRD, which gives averaged structural information. In the present investigation microstructures and morphology of raw and selected intercalated MMT were studied by TEM to compare the results with that of the XRD. TEM image of M showed interlayer spacing 1.10 - 1.20 nm (Figure 5) which closely resembled with XRD result. Bright field TEM images of M-Ph_3C_{12} and MBu_3C_{16} revealed well defined layer stacking separated by regular van der Waals gaps or galleries (Figure 6 and Figure 7). d-spacing values obtained from TEM images were 2.5 - 2.7 nm for M-Ph_3C_{12} and 2.1 - 2.3 nm for MBu_3C_{16}. Range of d-spacing value was observed rather than a

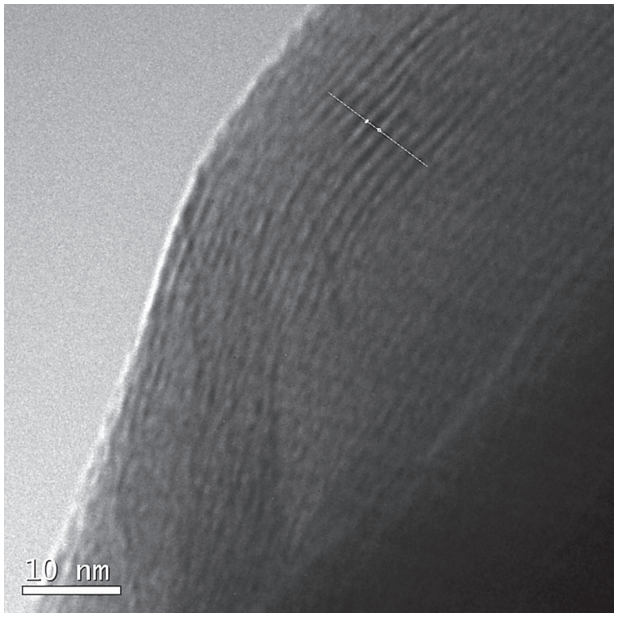

Figure 5. TEM image of M.

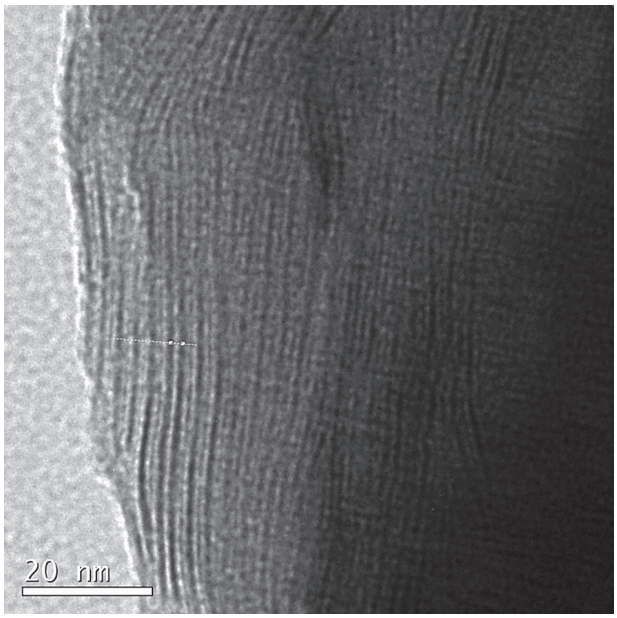

Figure 6. TEM image of M-Ph_3C_{12}.

Table 2. TG-DTG results of intercalated M.

Intercalated M	Peak temperature at 2nd stage mass loss (°C) (T_{max})	Peak temperature at 3rd stage mass loss (°C) (T_{max})	Mass loss at 2nd stage (wt. %)	Mass loss at 3rd stage (wt. %)	Organic loading (wt. %) (C-B)
M-Ph_3C_1	398	576	10	15	28
M-Ph_3C_2	353	582	7	14	28
M-Ph_3C_3	400, 466	565, 635	9	10	16
M-Ph_3C_{12}	325	550	12	16	34
M-Bu_3C_{14}	312	644	15	15	26
M-Bu_3C_{16}	330	478, 621	13	20	30
M-Bu_3C_4	387	598	7	7	9

single value which emphasized minor local variation due to layer stacking inhomogeneity. The local variation of d spacing from TEM supported the fact that different interlayer arrangements coexisted within interlayer space of MMT as evidenced by XRD results. However, the individual d spacing value from TEM study differed slightly with the XRD results (Table 3). These slight differences might be due to the influence of interlayer hydration on the d spacing of the MMT samples [31].

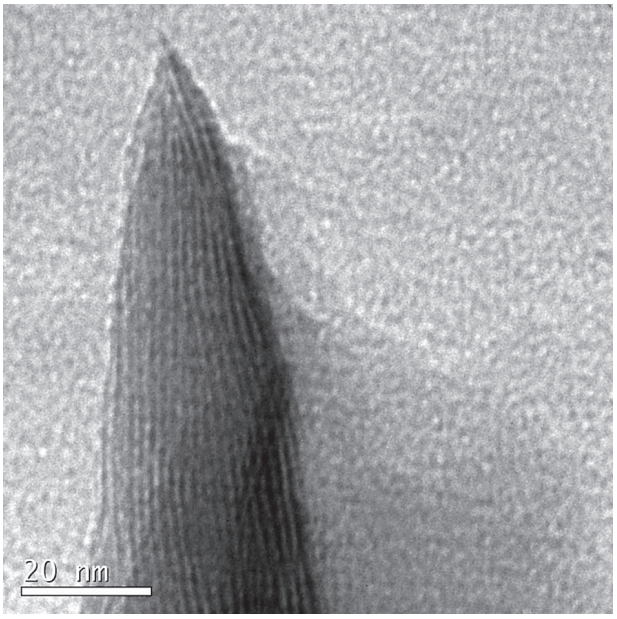

Figure 7. TEM image of M-Bu_3C_{16}.

Table 3. Comparison between d-spacings of XRD and HRTEM results.

Sample	TEM (d-spacing nm)	XRD (d-spacing nm)
M	1.1-1.2	1.25
M-Ph_3C_{12}	2.5-2.7	2.15, 2.7
M-Bu_3C_{16}	2.1-2.3	2.7

Thermogravimetric studies

Thermogravimetric studies of raw MMT indicated two major temperature regions of mass loss at around 200°C and 500 - 800°C which was the characteristic of such type of clay minerals [28]. The experimental clays and intercalated products were heat treated at 200°C to remove adsorbed moisture, so the plots have been drawn from 200°C (Figure 8). Intercalated MMTs showed another mass loss region within 300-500°C (Figure 9 and Figure 10). This mass loss was associated with organic decomposition [32-34]. DTG plots of intercalated MMT disclosed different mass loss peaks along with the peak temperatures (Figure 11 and Figure 12). The amount of mass loss associated with that temperature region was calculated from corresponding TG plot. The mass loss values at different stages with maximum peak decomposition temperature and organic loading (wt. %) has been furnished in the table (Table 2). As adsorbed water loss was excluded by heating the intercalated MMT at 200°C, further mass loss in the temperature region 300°C - 500°C was due to organic loss and loss above 500°C was due to structural water. If full intercalation was assumed, difference between total weight loss and structural water loss is an indicative of organic inclusion into the structure. So, organic loading (wt. %) was calculated by subtracting the structural water of M (heated at 200°C) from the total loss of intercalated MMT [33, 34]. Structural mass loss of M (heat treated at 200°C) within temperature region 500 - 800°C was observed to be ~ 4 wt. % (Figure 8). But losses at higher temperature range (500 - 750°C) of intercalated MMT were 10 - 15 wt.%. Higher temperature mass loss included structural water

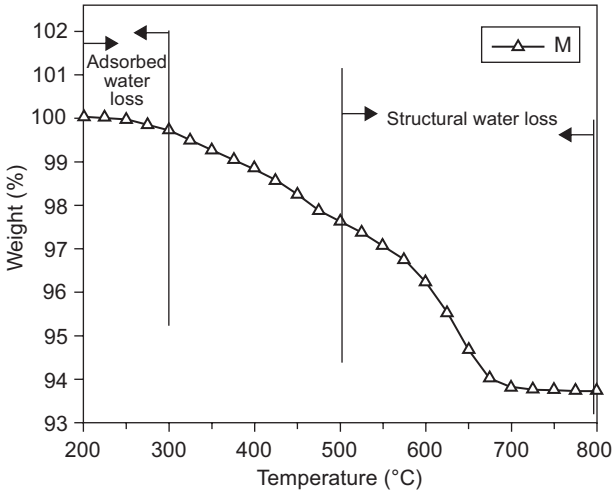

Figure 8. TG plot of M.

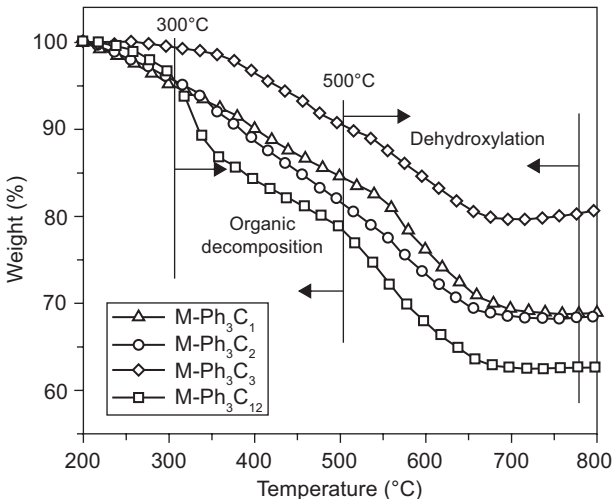

Figure 9. TG plot of alkyl triphenyl phosphonium salt intercalated MMT.

(4 wt. %) as well as residual organic components of the intercalated MMT which remain unaffected in 300 - 500°C. So, this higher temperature region of intercalated MMT was an overlapping mass loss region. Percent loss of material at two different stages was calculated (Table 2). Organic loading (wt. %) showed a general trend of increment with that of the alkyl chain length though M-Ph_3C_3 was exception which showed a low organic loading at 16 wt. %. Organic loading of M-Bu_3C_4 was also exceptionally low and the value was 9 wt. % only. The highest organic loading value was 34 wt. % of M-Ph_3C_{12} for triphenyl head group and 30 wt. % of M-Bu_3C_{16} for tributyl head group (Table 2). Results showed that highest organic loading was observed for the highest alkyl chain length in each group. Closer inspection of the DTG plots disclosed that with the increase of chain length, DTG peaks at higher temperature became more flattened for alkyl tributyl head group than those for alkyl triphenyl group (Figure 11 and 12). Flattened DTG peaks of intercalated MMT with alkyl tributyl phosphonium group indicated that decomposition was occurring over a wide temperature range. This might be due to higher tendency of tributyl phosphonium head towards pyrolysis than that of triphenyl phosphonium head which was internally more stable, after removal of long alkyl carbon chain in each case (Figure 13 and Figure 14). The sp^3 hybridized C–P bond in tributyl phosphonium easily undergoes fragmentation during pyrolysis to form more stable alkanes or olephenes which was not possible in sp^2 hybridized C–P bond in triphenyl phosphonium head. Internal stability of phenyl ring makes it disinclined towards fragmentation. So, decomposition of alkyl tributyl phosphoniums occurred over a wide temperature range following fragmentation pathway during heat treatment. The peak temperature associated with 2nd stage of mass loss (Organic loss) showed variation within the temperature range of 325 - 466°C for triphenyl phosphonium group and 312 - 387°C for tributyl group

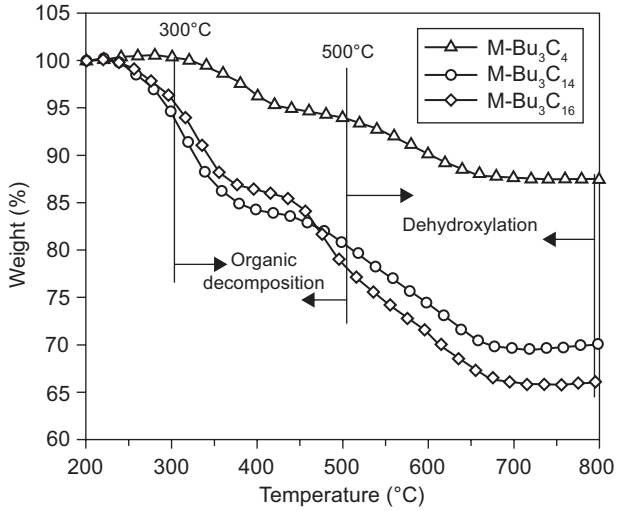

Figure 10. TG plot of alkyl tributyl phosphonium salt intercalated MMT.

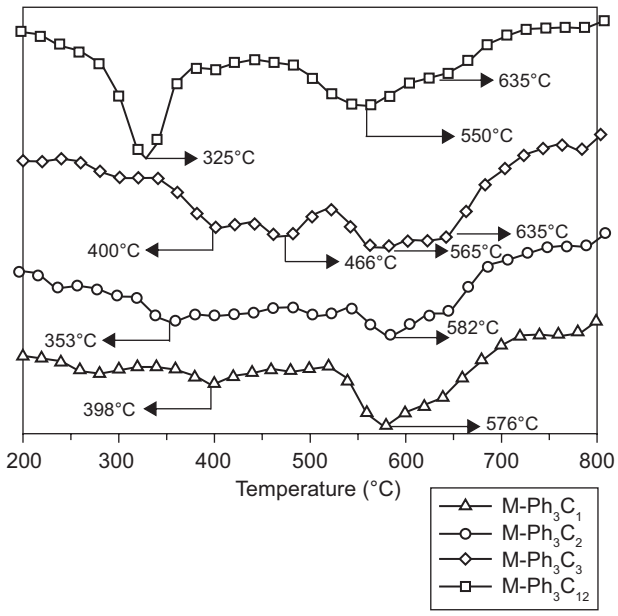

Figure 11. DTG plot of alkyl triphenyl phosphonium salt intercalated MMT.

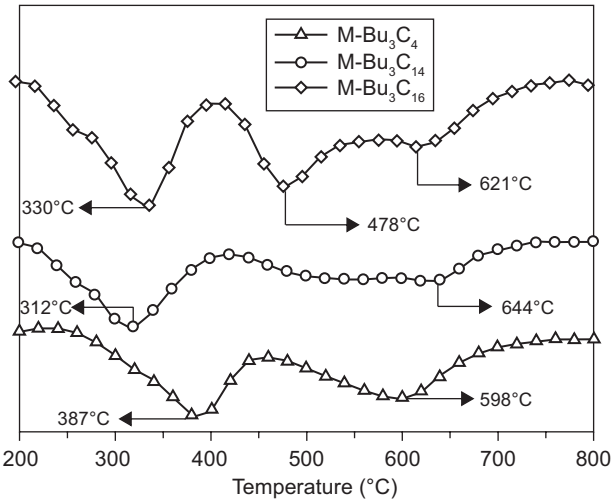

Figure 12. DTG plot of alkyl tributyl phosphonium salt intercalated MMT.

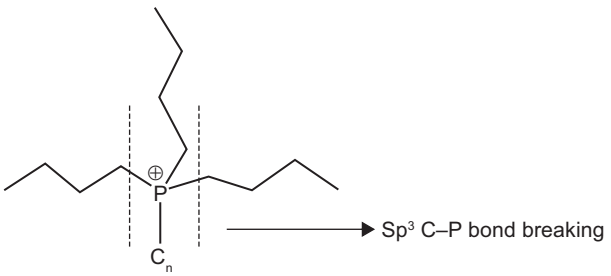

Figure 13. Structure of alkyl tributyl phosphonium head group.

of intercalates respectively (Table 2). Similarly 3rd stage of mass loss (organic and structural water loss) varied with in 550 - 582°C and 598 - 644°C for triphenyl and tributyl group of intercalates respectively (Table 2). Higher peak temperatures demonstrated higher energy for decomposition as well as higher van der Waals attachment within the organic cations.

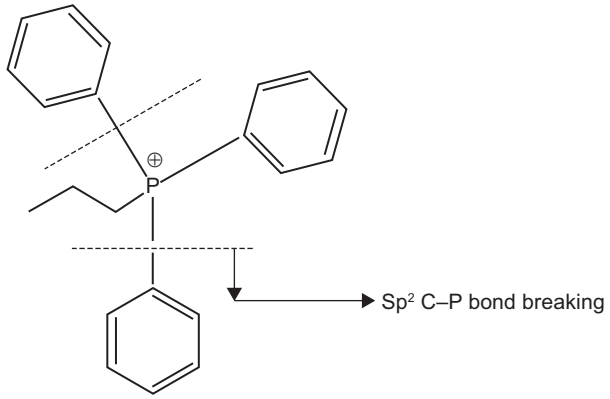

Figure 14. Structure of alkyl triphenyl phosphonium head group.

FTIR studies

FTIR plot of M (Figure 15) indicated the presence of both tetra coordinated and hexa coordinated aluminum along with Si–O linkages. [35]. Bands at 914 cm^{-1}, 879 cm^{-1}, 530 cm^{-1}, and 462 cm^{-1} were attributed to AlAlOH, AlMgOH, Si–O–Si, and Si–O–Al, bending vibrations, respectively. Similarly, peaks at 1035 cm^{-1} and 1116 cm^{-1} were characteristic for in plane and out of plane Si–O stretching [35-36] of MMT. Bands at 3697 cm^{-1} and 3628 cm^{-1} in the FTIR plot of M were due to –OH bond stretch for Si–OH and Al–OH group of MMT. The broad band centered near 3460 cm^{-1} was due to –OH stretching band for interlayer water. The overlaid absorption peaks in the region of 1645 cm^{-1} in the FTIR spectrum of M was attributed to –OH bending mode in adsorbed water. Alkyl triphenyl phosphonium intercalated MMT, as expected, indicated the presence of organic intercalates along with the characteristic bands for MMT (Figure 16). After intercalation, interlayer –OH bending and stretching modes (1636 cm^{-1}, 3460 cm^{-1}) were either absent or reduced to a negligible extent due to removal of interlayer water. Above said findings confirmed that MMT clay surface was hydrophobic in nature after intercalation. In IR spectrum of triphenyl phosphonium intercalated MMT, characteristic bands of the clay mineral were almost preserved with very little variation in the spectrum range due to organic inclusion (Figure 16). They showed a sharp peak at 1440 cm^{-1} for phenyl ring and at 3066 cm^{-1} for stretching of aromatic C–H bond. Bands at 2854 cm^{-1} and 2924 cm^{-1}, which were due to symmetric and asymmetric stretching of methylene group (–CH_2), were also present [37]. The frequency pattern in the lower frequency region (400 - 1500 cm^{-1}) of alkyl tributyl phosphonium intercalated MMT as demonstrated was a bit complex and altered to a considerable extent (Figure 17). The bands characteristic to bending vibration of Al–O and Si–O linkages were shifted as indicated in FTIR spectrum. This alteration of peak positions of Al–O or Si–O linkages occurred due to overlapping of characteristic peaks of organic intercalates with that of the structural clay mineral bands. Characteristic bands for symmetric and asymmetric stretching of methylene group (–CH_2) appeared at 2850 cm^{-1} and 2921 cm^{-1} which confirmed the intercalation of the molecule (Figure 17).

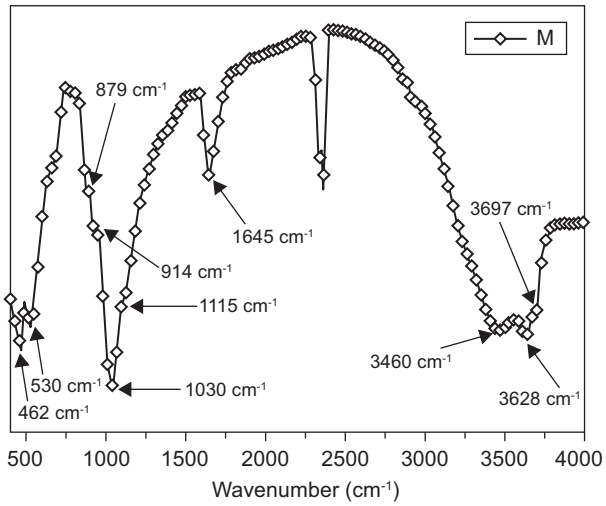

Figure 15. FFTIR plot of M.

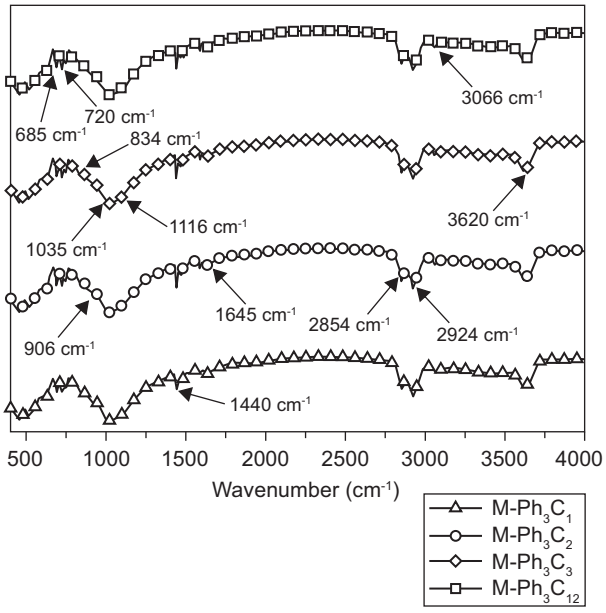

Figure 16. FTIR plot of Alkyl triphenyl phosphonium intercalated MMT.

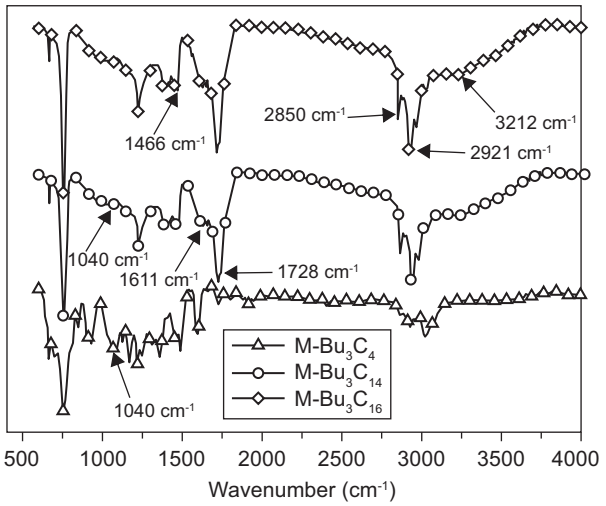

Figure 17. FTIR plot of Alkyl tributyl phosphonium intercalated MMT.

CONCLUSIONS

Interlayer spacing enhancements and interlayer arrangements of alkyl phosphonium intercalated MMT were influenced by alkyl chain length as well as effective volume occupied by cationic heads of incoming organic cations. Van der Waals interaction between alkyl chains of phosphonium cations was the guiding factor to influence interlayer stacking of organics and increment of organic loading. Decomposition mechanism of confined organics during heat treatment was different for different cationic head composition of alkyl phosphonium salts. Hybridization of bonds of different groups attached at the cationic head influenced the decomposition patterns. Hence decomposition peak pattern and peak temperature were altered with cationic head structures. FTIR analysis revealed that extensive overlapping of bands in lower frequency region (400 - 1500 cm^{-1}) was observed in alkyl tributyl phosphonium intercalated MMT which was absent in alkyl triphenyl intercalated MMT.

Acknowledgements

The work was supported by CSIR fellowship grant to Saheli Ganguly (currently working as senior research fellow in C.G.C.R.I., Kolkata). Authors would like to thank XRD, Instrumentation, TEM section of CGCRI for constant support.

References

1. Alexandre M., Dubois P.: Mater. Sci. Eng. R. *28*, 1 (2000).
2. Sinha Ray S., Okamoto M.: Prog. Polym. Sci. *28*, 1539 (2003).
3. Ruiz-Hitzky E., Aranda P., Serratosa J.M. in: *Handbook of Layered Materials*, p. 91-154, Marcel Dekker, New York 2004.
4. Bergaya F., Theng B.K.G., Lagaly G.: *Handbook of Clay Science* : *Developments in Clay Science*, Elsevier Ltd 2006.
5. Hrachova J., Komadel P., Chodak I.: Clays. Clay. Miner. *57*, 444 (2009).
6. Patel H.A., Somani R.S., Bajaj H.C., Jasra, R.V.: Bull. Mat. Sci. *29*, 133 (2006).
7. Maguy J., Lambert J.F.: J. Phys .Chem. Lett. *1***,** 85 (2010).
8. Emmerich K., Wolters F., Kahr G., Lagaly G.: Clays. Clay Miner. *57*, 104 (2009).
9. Gu Z., Guajon S., Liu S.Y., Gao J.: Clays. Clay Miner. *58*, 72 (2010).
10. Kaufhold S., Dohrmann R., Klinkenberg M.: Clays. Clay Miner. *58*, 37 (2010).
11. Liang H.N., Long Z., Zhang H., Yang S.H.: Clays. Clay Miner. *58*, 311 (2010).
12. Li Z., Kolb V.M., Jiang W.T., Hong H.: Clays. Clay Miner. *58*, 462 (2010).
13. Erkan I., Alp I., Celik, M.S.: Clays. Clay Miner. *58*, 792 (2011).
14. Morodome S., Kawamura K.: Clays. Clay Miner. *59*, 165 (2011).
15. Xie W., Gao Z., Pan W. P., Hunter D., Singh A., Vaia R.: Chem. Mater. *13***,** 2979 (2001).
16. Davis C.H., Mathias L.J., Gilman J.W., Schiraldi D.A.: J. Polym. Sci. Part B: Polym. Phys. *40*, 2661 (2002).
17. Gilman J.W., Awad W.H., Davis R.D., Shields J., Harris H.R., Davis C., Morgan A.B., Sutto T.E., Callahan J., Trulove P.C., Delong H.C.: Chem. Mater., *14*, 3776 (2002).
18. Xie W., Xie R., Pan W. P., Hunter D., Koene B., Tan L.S., Vaia R.: Chem. Mater. *14*, 4837 (2002).
19. Patel H.A., Somani R.S., Bajaj H.C., Jasra, R.V.: Appl. Clay. Sci. *35*, 194 (2007).
20. Avalos F., Ortiz J.C., Zitzumbo R., Manchado M.A.L.., Verdejo R., Arroyo, M.: Appl. Clay. Sci. *43*, 27 (2009).
21. Liu X., Lu X., Wang R., Zhou H., Xu S.: Clays. Clay. Miner. *55*, 6, 554 (2007).
22. Li Z., Jhang W.T.: Clays. Clay Miner. *57*, 194 (2009).
23. Mehlich A.: Soil Sci. *66*, 429 (1948).
24. Bache B.W.: J. Sci. Food. Agri. *27*, 273 (1976).
25. Hillier S., Clayton T.: Clay Miner. *27***,** 379 (1992).
26. Bergaya F., Lagaly G., Vayer M. in: *Handbook of Clay Science,* p. 979-1001 ed. Bergaya F., Theng B.K.G., Lagaly G., Developments in Clay Science, Elsevier Ltd 2006.
27. Grim R.E.: *Clay Mineralogy*, McGraw-Hill 1968.
28. Theng, B.K.G.: *The Chemistry of Clay-Organic Reactions*. Wiley-interscience, New York 1974 .
29. Lagaly G., Beneke K., Weiss A.: Am. Mineral. *60*, 642 (1975).
30. Favre H., Lagaly G.: Clay Miner. *26*, 19 (1991).
31. Marcovich D.Y., Chen Y., Nir S., Prost, R.: Environ. Sci. Tech. *39*, 1231 (2005).
32. Ganguly S., Dana K., Ghatak S.: J. Therm. Anal. Calorim. *100*, 71 (2010).
33. Ganguly S., Dana K., Mukhopadhyay T.K., Ghatak S.: Clays. Clay Miner. *59*, 13 (2011).
34. Ganguly S, Dana K, Mukhopadhyay T.K., Ghatak S.: J. Therm. Anal. Calorim. *105*, 199 (2011).
35. Farmer, V.C.: *Infrared Spectra of Minerals*, p.331, Mineralogical Society, London 1974.
36. Madejova J.: Vib. Spectrosc. *31***,** 1 (2003).
37. Dyer, J.R.: *Applications of absorption spectroscopy of organic compounds*, Prentice-Hall International. Inc., Englewood Cliffs., New York 1965.